A review of totally implantable wireless ultrasonic Doppler blood flowmeters: towards accurate miniaturized chronic monitors

Michael A. Rothfuss[a], Jignesh V. Unadkat[b], Michael L. Gimbel[b], Marlin H. Mickle[a], Ervin Sejdić[a,*]

[a]*Department of Electrical and Computer Engineering, Swanson School of Engineering, University of Pittsburgh, Pittsburgh, PA, USA.*
[b]*Department of Plastic Surgery, University of Pittsburgh, Pittsburgh, PA, USA.*

Abstract

Totally implantable wireless ultrasonic blood flow meters provide direct-access chronic vessel monitoring in hard-to-reach places without using wired bedside monitors or imaging equipment. While the accuracy of wireless implantable Doppler devices satisfies most applications, device size and implant lifetime remain vastly underdeveloped. This paper reviews past and current approaches to miniaturization and implant lifetime extension for wireless implantable Doppler devices, and it proposes approaches to reduce device size and maximize implant lifetime for the next generation of devices. Additionally, this paper reviews current and past approaches to accurate blood flow measurements. This review points towards relying on increased levels of monolithic customization and integration to reduce size. Meanwhile, recommendations to maximize implant lifetime should pursue alternative sources of power, such as transcutaneous wireless power, which stand to extend

*Corresponding Author: Ervin Sejdić, 3700 O'Hara St. Benedum Hall Room 1238 Pittsburgh, PA 15261; E-mail: esejdic@pitt.edu, Phone: 412-624-8003

lifetime indefinitely. Coupling together the results will pave the way for ultra-miniaturized totally implantable wireless blood flow monitors for truly chronic implantation.
Keywords: Batteryless, blood flow monitor, flowmeter, free flap, wireless power, transcutaneous wireless power

---

Introduction

Microvascular free flap (MFF) surgeries are a class of procedures used in reconstructive surgeries to correct anatomic defects requiring persistent monitoring to ensure surgical success (Hong et al., 2014; Zhou et al., 2014; Kang et al., 2013). MFF surgeries involve the transfer of a tissue block (i.e., flap) from one part of the body (e.g., thigh, buttocks) to another (e.g., breast, mandible). The arteries, veins, and other connective tissues of the donor tissue are connected to those at the transfer site. The microvascular connections, called anastomoses, establish blood flow to the transferred tissue block (O'Brien et al., 1974; Goodstein and Buncke Jr, 1979). Anastomotic failures (i.e., due to clotting, leaks, etc.) hinder blood flow to the transferred tissue. Unless these failures are caught, the tissue will certainly die (Chen et al., 2007; Wu et al., 2013). MFF monitoring by trained technicians is a necessity to reduce the death of tissue and subsequent risky surgical re-exploration. Of the many MFF monitoring technologies available, few can provide an accurate, easy-to-use, and cost effective combination.

All MFF monitoring techniques need to be accurate, and false-positives and false-negatives lead to costly and risky surgical re-exploration. Ease-of-use can be a limiting factor in a monitoring technology's adoption, particularly when the technology requires skilled technicians and prevents patient mobility. Early and quick detection (i.e., through monitoring) of the nearly 10% to 20% of compromised vessels in free flaps has helped to increase flap salvage rates (Yu et al., 2009; Liu et al., 2012), which has lead to the continued development and exploration of numerous monitoring technologies to minimize lost flaps.

Techniques to monitor MFFs are abundant, but many have fallen to disuse in favor of cheaper and more practical and easier to use alternatives that can service the gamut of applications. Buried flaps, vascularized bone grafts, pigmented skin flaps, skin grafted muscle flaps, and flaps with small skin paddles are all challenges that a monitor must face with evaluation. Several monitors, such as the fluorescein monitor, thermocouple, photoplethysmography, the transcutaneous laser Doppler, and the transcutaneous Po_2 monitor have significant drawbacks which have lead to their disuse (Swartz et al., 1988). Non-invasive near-infrared spectroscopy (NIRS) showed promise with its low false-positive and low false-negative rates. However NIRS monitoring suffers from several drawbacks, which include: a slow response time, an inability to monitor buried flaps, a sensitivity to interfering light sources, and finally, it is cumbersome (Lohman et al., 2013). Even newer monitoring methods such as positron emission tomography (Schrey et al., 2008) and microendoscopy (Upile et al., 2006), are considered cumbersome and impractical. The Cook-Swartz implantable Doppler device, however, offers significant advantages over its competitors. This device allows for direct-contact monitoring of a vessel, which increases the reliability of patency monitoring, particularly for buried free flaps (Disa et al., 1999).

Even though the wired implantable Doppler is considered the gold standard in MFF monitoring (Guillemaud et al., 2008; Pryor et al., 2006; Oliver et al., 2005; Rozen et al., 2011), it is not without its shortcomings (Cho et al., 2002; Rosenberg et al., 2006; Paydar et al., 2010), which can be mitigated through the employment of another Doppler technology, the wireless implantable Doppler (WID) (Rothfuss et al., 2016; Gimbel et al., 2014; Un-

adkat et al., 2014). This paper will focus on *totally* implantable WID devices using piezoelectric transducers. The review excludes multi-channel and multi-sensor devices (e.g., (Axelsson et al., 2007; Gräns et al., 2009; Kong et al., 2005)), due to their additional size and power consumption, precluding comparisons with other WIDs. The paper will review the major open problems towards developing WIDs for MFF and chronic implantation applications. Published solutions to these problems and the emerging and future directions to solve these problems will follow.

Clinical Blood Flow Monitoring: A Background

Elements of an Ideal Monitor

The ideal microvascular blood flow monitor is easily deployable and easily interpretable by inexperienced operators, provides continuous and reliable monitoring, tolerated by the patient, and applicable to any site, (Smit et al., 2010). To date, according to Smit et al., the most promising monitors for free flap monitoring are the Cook-Swartz wired implantable Doppler, near-infrared spectroscopy, and Laser Doppler flowmetry. While NIRS and Laser Doppler flowmetry are non-invasive and reliable, they are not applicable to all sites nor easily interpretable like the wired implantable Doppler. However, the wired implantable Doppler suffers from reliability problems. No single technology has achieved these specifications fully, and has left the field open for solutions.

In anastomoses cases, deployment simplicity and monitoring reliability have been addressed by using anastomotic flow couplers (Zhang et al., 2012). Major reliability problems with the wired Doppler probe stem from probe

placement, for which proper placement requires experience (Yu et al., 2009). The flow coupler conveniently incorporates the probe into the coupler's rigid ring wall to reduce the placement difficulties. The flow coupler can be rapidly deployed using a hand-held assembly. Recently, monitors have targeted the reliability problems and interpretation difficulties of the wired Doppler gold standard, which stem from its wire tether to a bedside monitor and lead to additional unnecessary surgery (Zhang et al., 2012), by eliminating the problematic wire tether and totally implanting the monitor (Unadkat et al., 2015; Rothfuss et al., 2016). True continuous monitoring requires an unlimited power source, which is only currently found in bedside monitoring (i.e., those using wall outlets). In power constrained applications (i.e., totally implanted wireless monitors), approximately continuous monitoring has been demonstrated by duty-cycling the implant power-on/sensing time (Vilkomerson et al., 2008; Cannata et al., 2012; Rothfuss et al., 2016), often achieving years of approximately continuous measurement.

Invasive technologies, such as the implantable wired Doppler, are only tolerable in the short-term, due to limiting patient mobility. To-date, all totally implantable blood flow monitors remain overly large and intolerable to patients. The root of the non-ideal implants sizes is shared among: lack of advanced monolithic integration (e.g., (Gill and Meindl, 1975; Di Pietro and Meindl, 1978), power requirements (e.g., battery size (Yonezawa et al., 1992; Vilkomerson et al., 2008; Rothfuss et al., 2016)), and implant antenna size (e.g., telemetry (Vilkomerson et al., 2008) and/or wireless power transfer (Tang et al., 2014)).

Economics of Monitoring and Failures

The financial aspects of free flap monitoring, and cost associated with surgical reexploration represent a barrier towards a monitoring technology's adoption. When free flap failure occurs, the financial costs are high. Fischer et al.'s cost analysis for breast flaps, across 1303 flaps between 2005−2011, showed major surgical complications increased the length of stay to 6.14 days on average with a total average cost of $28,261, compared to no complications, which incurred 4.20 days on average and an average cost of $19,106. A cost penalty of $9,155 and an increased stay of 1.94 days. For head and neck flaps, Gupta's 2010 analysis (in $CAD) showed failed flaps cost $1413.73/day for an average stay length of 34.5 days; compared to $1327.71/day for an 18.8 day stay in successful free flap surgeries (Gupta, 2012), a difference of $23,812.74 more for failures. Dollar amounts in Gupta's analysis were converted from Canadian Dollars to U.S. Dollars from the 2010 Canadian-to-U.S. exchange rate of 1.072 as published by the Internal Revenue Service (IRS) (Service, 2016).

Another financial aspect of the monitoring period is the cost of the monitoring device, which vary by many factors, including, accuracy, applicability, ease-of-use, invasiveness, amongst others. Here, we discuss the results of Smit et al.'s review of popular monitoring modalities (Smit et al., 2010). Of the available monitors, the best are the implantable Doppler, the near-infrared spectroscopy, and the laser Doppler flow meter. The implantable Doppler is the cheapest (i.e., $3100 monitor + $412 disposable probes), followed by laser Doppler flowmetry (i.e., $5460 + $1050 per 10 probes), and then NIRS (i.e., $16.5k+ $150 sensors). Other valuable monitors include the familiar

color duplex ultrasound machines and microdialysis. However, their cost is significant compared with the three best monitoring choices (i.e., color duplex: \$30k−\$225k; microdialysis: \$52k analyzer + \$570 consumables). While NIRS and Laser Doppler flowmetry are both noninvasive and have 100% positive and negative predictive values, their penetration depth is limited and cannot be used for deeply buried flaps (i.e., 20 mm max for NIRS and 8mm max for Laser Doppler). Despite having a lower positive predictive value than NIRS and Laser Doppler flowmetry, the implantable Doppler flow meter can monitor all flap types, including buried flaps, and can be interpreted by minimally trained or unexperienced personnel, and is considered a simpler technique to use compared to NIRS and Laser Doppler flowmetry. The implantable wireless blood flow monitors stand to improve the adoption of the Doppler monitoring technique by eliminating the root of the wired implantable Doppler's imperfect positive predictive value − the transcutaneous wire to the bedside monitor. Cost estimates of the wireless implantable Doppler have yet to be reported in literature.

Clinical and Research Need Summary

While no single monitor is fits the ideal mould, the closest candidates reported in literature are the wired implantable Doppler, near-infrared spectroscopy, and Laser Doppler flowmetry. Compared these methods, the implantable Doppler is the only invasive modality, with the exception that microdialysis is minimally invasive. Table b summarizes the blood flow monitoring modalities along with their clinical advantages and disadvantages.

The wired implantable Doppler stands out from others as it provides immediate feedback, is easily interpreted by inexperienced personnel, and can

be used with any type of flap, including buried flaps. The wired implantable Doppler implantation process requires direct vascular access, which is the root of the technology's success across all flaps; the transcutaneous wire connects the bedside monitor to the sensor affixed to the vessel. After the post-monitoring period, the wire is tugged and breaks free from the sensor and cuff at the vessel site, which remain in the patient permanently. This wire is the source of the implantable Doppler's shortcomings and amounts to reduced reliability, potential for injury, and unnecessary surgeries. The major problems associated with the transcutaneous wire are described by Yu et al. (Yu et al., 2009), Zhang et al. (Zhang et al., 2012), and Kempton et al. (Kempton et al., 2015) and are summarized below:

- Limited patient mobility which increases the risk of vessel kinking and damage.
- Easily dislodged internally, resulting in high false-positives and expensive and unnecessary surgical re-exploration.
- Tenuous and cumbersome to have in the operative field after placement, due to the potential for inadvertent snagging and dislodgement or injury.
- Potential for injury to vessels upon removal at the end of the monitoring period.

Until recently, the body of literature had not investigated the wireless implantable Dopplers as a competitor to the wired device. Even if future

studies confirm the efficacy of the wireless Doppler, the focus of wireless implantable Doppler literature has been more on accuracy and implant lifetime rather than the more practical aspects of an implantable monitor, namely its size. The wireless implantable Doppler technology, likewise to the wired implantable Doppler, is intended to remain inside the patient both during and after the free flap monitoring period. Its size is paramount, which directly affects patient tolerability. Literature frequently focuses on wireless implantable Dopplers as chronic monitors. Besides implant size, the power source is predominantly batteries, which are bulky and have limited lifetimes, even if rechargeable. Two worthwhile candidates for providing sufficient and unlimited power to implants in a small size are transcutaneous wireless power and ultrasonic wireless power. To date, literature has not focused on solutions to extending implant lifetime using these inexhaustible sources of power, which stand to not only extend the implant lifetime indefinitely but also reduce implant size, making a more ideal monitor.

Wireless restenosis monitoring after stent placement has been an active area of research since 2003, and represents a chronic monitoring application for wireless blood flow monitors. Restenosis is the intraluminal re-narrowing of a revascularized vessel to treat atherosclerosis (i.e., the accumulation of plaque in arterial walls). As an example application, when atherosclerosis occurs in the lower-limb arteries, it is called Peripheral Artery Disease (PAD). PAD is asymptomatic in $20-50\%$ of those with the disease (McDermott et al., 2008), and nearly 50% of cases experience complications within the first year after revascularization. Three years after stent deployment, about $63-66\%$ of vessels remain patent (Muradin et al., 2001). Currently, patients

visit hospitals every 3 to 6 months to detect restenosis (Radermacher et al., 2001); a wireless restenosis monitor stands to eliminate the need for hospital visits, saving hospitals money and improving patient compliance.

In wireless restenosis monitoring, the stent is used as an antenna (Keikhosravy et al., 2012, 2014). Current methods of wireless restenosis monitoring either use changes in tissue properties that de-tune the antenna (Occhiuzzi et al., 2011, 2012) (i.e., the degree of detuning is sensed) or a blood pressure sensor (Takahata et al., 2003, 2006; DeHennis and Wise, 2006; Chow et al., 2010). However, no wireless restenosis monitor has been reported to monitor blood flow using the Doppler technique. Despite this gap in literature, during hospital visits, duplex Doppler ultrasound imaging of the diseased vessel is performed, leading to the conclusion that a Doppler blood flow monitor incorporated into the stent antenna would provide meaningful and familiar modality. The degree of renarrowing is clearly evident as increased turbulent flow (Nelson and Pretor, 1988; Arger and Iyoob, 2004), showing a significantly broader Doppler spectrum as renarrowing worsens and as much as a 100% peak velocity increase, according to Guo et al. (Guo et al., 1994). Development of an implantable wireless chronic blood flow monitor would allow for at-home treatment and reduced hospital costs for the nearly 5 million American adults in the U.S. with PAD (Selvin and Erlinger, 2004).

Mechanisms of Doppler Ultrasound and Accuracy

In 1961, Franklin et al. showed that blood flow could be measured by exploiting the Doppler effect with ultrasonic backscattering (Franklin et al., 1961). This was the first report of blood flow measurement using the Doppler

effect. This device had direct access to the vessel, and the accuracy was reported as 5% of the full scale 100 cm/s. The design was simple and inexpensive, and its frequency meter output was linearly related to the instantaneous flow velocity. Therefore, the mean Doppler shift frequency is proportional to the instantaneous blood flow velocity.

There are two major Doppler ultrasound configurations for blood flow measurements. The first is the continuous wave (CW) Doppler configuration, and the second is the pulsed wave (PW) Doppler configuration (Shung, 2005). Both configurations have varying degrees of accuracy depending on the application environment (i.e., flow characteristics, inner lumen diameter, inner lumen shape) and measurement assumptions. A full treatment of error sources and measurement assumptions involved in Doppler ultrasound blood flow determination are described by Gill (Gill, 1985).

Figure 2 shows a representative system-level CW Doppler flowmeter block diagram. The high-voltage (HV) driver excites the transmitting transducer, and a high frequency (HF) low-noise amplifier connected to the receiving transducer amplifies the weak echoes from tissue and blood. The echoes are demodulated down to baseband. The sample volume of the CW Doppler is fixed, and therefore, if the sample volume is too large for the application, then the origin of echoes may come from outside the intended target area as illustrated in the figure. Conversely, if the sample volume is too small (i.e., small relative to the lumen cross sectional area), only a uniform flow profile (i.e., plug flow) can be accurately measured because complex flows types will exhibit dissimilar flow outside of the small sample volume. This notion exposes a limitation of the CW Doppler device: it cannot determine the origin

of the echoes in a vessel. The poor spatial resolution means that accurate assessment of volumetric flow is degraded in many blood flow environments.

A representative system-level block diagram of the PW Doppler flowmeter is shown in Figure 1. It uses an HV drive in a pulsed excitation. During lulls between pulses, created by using the transmit/receive (TX/RX) switch for blocking, received echoes across the vessel lumen (i.e., at various depths) are amplified using a time gain compensation amplifier, followed by demodulation to baseband. The PW configuration takes flow measurements in small incremental cross-sectional areas. The volumetric flow equals the sum of the product of each cross-sectional areas with the velocity within each cross-sectional area. The PW Doppler is constrained by an upper blood flow velocity limit. That is to say, the highest resolvable Doppler frequency is limited by the PW Doppler's pulse repetition frequency (PRF).

A popular alternative flow metering modality, to the Doppler ultrasound technique used in wireless Doppler blood flow meters, is the transit-time ultrasonic technique. This technique uses two transducers mounted on opposite sides of the vessel at an angle to the vessel wall. Ultrasonic pulses are transmitted from one transducer and received by the other, and then the transmitter/receiver roles are switched, leading to an upstream and downstream flow measurement. The time difference of the two transit-times provides an accurate measure of the average fluid velocity that is invariant to many parameters, which significantly affect the ultrasonic Doppler flow meter (Gill, 1985), including internal/external vessel diameter and shape, transducer angle θ, according to D'Ancona et al. (D'Ancona et al., 1999).

At first, the transit-time flow meter would appear superior to the Doppler

ultrasound flowmeter; however, a practical problem with the transit-time flow meters is that the resulting time-difference is very small, on the order of 10^{-9}s, and electronics to extract the time difference are complex (Webster, 1998). If a low enough insonifying frequency is used, the phase difference provides a measure of the time-difference. However, without accurate knowledge of the transmitter/receiver phase relationships, and unlike the Doppler ultrasound flow meter, the problem of zero-drift for the baseline zero-flow arises, when parameters such as transducer impedance change, according to Meindl (Meindl, 1972). Phase compensation after implantation increases the complexity, and thus power consumption of the design. Still, also according to Meindl, the transit-time flow meter suffers from flow ambiguity problems, where different velocity profiles can result in the same average velocity, thereby requiring *in situ* user calibration for volume flow (Meindl, 1972). The limitations of the transit-time technique (i.e., complexity, stability, user calibration) have clearly impeded its adoption in the body of published literature for wireless implantable blood flow meters. To the best of the authors' knowledge, there have been no reported wireless blood flow monitors using the transit-time principle.

Wireless Implantable Doppler Devices

Continuous Wave

Shortly after Franklin demonstrated the use of the Doppler effect to measure blood flow in 1961 (Franklin et al., 1961), Franklin et al. reported a wireless implantable CW Doppler device in 1964 (Franklin, 1964). However, while the blood flow data were reported wirelessly, the device was not totally implantable and the bulk of the equipment was worn in a harness or a helmet.

This same wireless implantable CW device developed by Franklin et al. was later benchmarked to report important findings related to accuracy (Franklin et al., 1965): (1) the Doppler frequency shift shows a linear relationship with blood flow, (2) flow can be determined accurately using the frequency shift when the vessel lumen area remains constant, (3) pulsatile flow that modifies the vessel lumen area decreases the accuracy by distorting the linear relationship, (4) using the zero crossing counter technique for detecting frequency shift is inaccurate for pulsatile jet-like flows, particularly because of the loss of directional flow information using this technique, and (5) this particular device could not resolve flow below 1 cm/sec because of the 40 Hz lower-limit of the implemented signal processing amplifier bandwidth.

Theoretical analysis and optimal designs of CW Doppler flowmeters and CW WID flowmeters began to appear in literature about a decade after Franklin et al.'s original work. Key system parameters and system trade-offs were discussed by Gill et al. (Gill and Meindl, 1973), which include ultrasonic frequency, burst repetition frequency, transducer diameter, transducer angle, and burst length (i.e., in the case of PW Doppler devices), along with appropriate electronic filters, amplifiers, and radio telemetry. Theoretical analysis of the CW Doppler flow meter reported by Brody et al.(Brody and Meindl, 1974) leveraged the development of an optimal system design for a totally implantable CW WID device, by DiPietro et al. (Di Pietro and Meindl, 1978). Using a zero crossing counter (ZCC), which estimates the mean Doppler frequency shift (Shung, 2005), DiPietro et al. reported good accuracy (i.e., $\pm 20\%$ from theory) for center velocity regardless of lumen diameter or flow profile (i.e., provided the sample volume is small relative

to the vessel diameter). However, accurate flow volume estimation still remained out of reach due to the uncertainty of flow profile across the lumen. Additionally, the ZCC accuracy is known to decrease if the bandwidth of the Doppler spectrum is wide and if the signal-to-noise ratio is poor (Gill, 1985).

In the late 1980s and early 1990s, further reports of wireless implantable Doppler devices appeared in literature. In 1989, Yonezawa et al. reported a nondirectional miniaturized CW Doppler device. (Yonezawa et al., 1989). This device utilized a ZCC to determine blood flow (i.e., relating the mean Doppler shift frequency to flow velocity via the Doppler equation). Though the device was intended for a backpack, suggestions for reducing the size for total implantation were given. Later on in 1992, Yonezawa et al. developed a directional wireless CW device (Yonezawa et al., 1992). Although this device was also not entirely implantable (i.e., the electronics connected to the transducers via transcutaneous leads), its design hinged off of his previous work, which could be implanted with Yonezawa's suggestions. This work in 1992 used a method of sensing directional information which differed from its predecessors. This method employed two phase-shifted versions of the totally implantable nondirectional CW flowmeters previously developed by Yonezawa to obtain one low-frequency directional reference signal and one standard Doppler audio signal. Flow was tested *in vitro* over 20 cm/s $-$ 150 cm/s flow rates, and the flowmeter output linearity was within $\pm 1\%$ to the actual value.

In the new millennium, the CW WID devices turned towards the chronic monitoring of vascular grafts. Within three years, with monitoring and subsequent correction, 20% of vascular grafts are no longer patent; with-

out monitoring, 45% are not patent. Vilkomerson et al. developed a directional CW WID to chronically monitor these vascular grafts, with an average blood flow velocity accuracy error less than 5% (Vilkomerson and Chilipka, 2004; Vilkomerson et al., 2008). The accuracy was achieved using ultrasonic double-beam diffraction grating transducers (DGT) (See Section: "Diffraction Grating Transducers"), which enabled angle independent blood flow measurements. Transducer angle was previously reported as a critical system parameter by Gill et al. (Gill and Meindl, 1973), which makes the double-beam DGT a significant advantage over conventional CW and PW transducer configurations. Later work by Vilkomerson et al. achieved average blood flow velocity accuracy errors less than 6%, and a peak blood flow velocity measurement deviating only 1.7% from measurements performed with a duplex ultrasound system (Cannata et al., 2012). Compared to the earlier work, which used a double-beam DGT embedded in a graft wall and operating at an ultrasonic frequency of 20 MHz, this work featured a flexible DGT operating at 40 MHz, which could be wrapped around a vessel for monitoring. Yet another DGT-enabled WID was developed and demonstrated by Tang et al. (Tang et al., 2014); however, unlike previous WIDs developed for chronic implantation since the turn of the century, this WID contained a small rechargeable battery, which is charged by transcutaneous wireless inductive powering. This device operated with a 30 MHz ultrasonic frequency. Power was delivered to the implant in order to charge a lithium polymer battery for 20 seconds, which provided 5 seconds of blood flow monitoring time. Reports of device accuracy were only available for one measurement (i.e., the peak Doppler shift frequency was equated to a flow rate); compared

to a volumetric flow measurement of 24 cm/s, Tang et al. reported 22.6 cm/s flow rate with their device.

Also since the turn of the century, research into occlusive/patency WID monitors for MFFs were demonstrated by Rothfuss et. al (Rothfuss et al., 2016) and Unadkat et. al. (Unadkat et al., 2014, 2015) and Gimbel et al. (Gimbel et al., 2014). The authors' device focused on the detection of binary flow states (i.e., flow or no flow). This means that the WID establishes the no flow (i.e., indicative of an occlusion) baseline in order to compare it with subsequent flow measurements. The device was calibrated *in vitro* reporting an accuracy of $< \pm 5\%$ above 8.00 mL/min and between -0.8% and 1.2% at the largest calibrated range. Venous occlusions were reproducibly detected in bilateral femoral veins in pigs across 32 trials.

Pulsed Wave

As described by Allen et al. (Allen et al., 1977), the first mention of a PW Doppler blood flowmeter was in 1969 (Peronneau and Leger, 1969; Wells, 1969; Baker, 1970). Gill et al. (Gill et al., 1971) and McLeod et al. (McLeod and Anliker, 1971) (as cited by Allen (Allen et al., 1977)) were also responsible for early developments with PW Doppler devices, but it was Gill's work that directly lead to a number of future developments incorporating his work.

The PW WID was first described by Gill (Gill and Meindl, 1973), and the optimal system parameters for the PW WID design were discussed. The preliminary *in vitro* experiments with Gill's PW WID showed a $\pm 15\%$ blood flow volume estimation (Gill and Meindl, 1975). Soon after the development of Gill's PW WID, a nondirectional PW WID was demonstrated by Henry

et al. (Allen et al., 1977), which could sample eight velocity points across its cuff − 11 mm inner diameter. Over 77 trials, the accuracy was +2.0 ±8.7%, showing improvement over the first PW WID demonstrated by Gill in 1975. It was suggested that the accuracy overestimation was due to slight variations in the transducer angle. Allen et al. later reported circuits for a bidirectional PW WID to improve upon the accuracy of the previously developed nondirectional PW WIDs (Allen et al., 1978). However, no accuracy measurements were reported for this device. Additionally, a unique variation of a PW WID, compared to other reported PW WID devices, was demonstrated shortly after Gill's first report on PW WIDs by Hartley et al. (Hartley and Cole, 1974). This unique variation accomplished chronic implantation by transcutaneous wireless excitation of the probe itself. That is to say, the leads of the probe were formed into a coil near the surface of the skin prior to surgical closure of the animal, and an external coil magnetically couples to the implanted probe. In this study, probes were calibrated for each vessel to remove the typical uncertainties in lumen center velocity, lumen diameter, and crystal alignment.

In recent years, an inductive/magnetic powering or power delivery purposed for or to a WID has been developed. Tang et al. reported an ultrasonic pulser that could be magnetically powered (Tang et al., 2011); although, the device was not tested in animals and no blood flow accuracy data were reported, their device is described as a potential candidate for future studies that measure blood flow. The device may show promise as a chronically implantable device if its accuracy is acceptable.

Doppler Ultrasound Accuracy Summary

Since the development of implantable Doppler blood flow monitors in the early and late 1960s, there has been significant attention towards improving their accuracy. By understanding the sources of error, new techniques were developed and incorporated into the Doppler devices, such as ZCCs, directional flow measurements, range-gated pulse-wave measurements, uniform insonification, etc. For example, directional flow monitors improve upon nondirectional monitors because for flow situations exhibiting flow reversal, such as in the splenic vein or variations with the cardiac cycle in the aorta. Ignoring the direction of flow will give an inaccurate understanding of the flow characteristics. To expound on another example, the range-gated pulse-wave WID devices solve the problem of unknown vessel dimensions and lumen diameter, which vary across measurement site and subject. The range-gated pulse-wave WID can selectively resolve flow at specific ranges away from the transducer face, thereby obtaining high spatial resolution for accurate flow profile assessment and accounting for variations in vascular dimensions.

Table b summarizes major WID devices reported in literature along with their reported accuracy. From the table, it is noted that the PW WID devices demonstrate greater accuracy for the blood flow rate in a vessel, compared with the CW WID devices. This is explained by the fact that PW WID devices measure flow at various sample volumes across the entire vessel lumen, which provides information about the flow profile of blood flow in a vessel. Additionally, the directional flowmeters generally show better accuracy over the nondirectional flowmeters.

Miniaturization

Device size is a critical metric WID devices throughout literature. The size of a device imposes a foreign body response by the host (Morais et al., 2010). A large implanted device can cause patient discomfort and may be impractical.

Commercial Off-the-shelf

Commercial off-the-shelf (COTS) parts are a practical and convenient way to satisfy quick development schedules, develop proof-of-concepts, and perform exploratory research at a low cost. Many studies reported in literature with WIDs, both CW and PW, are either mostly or completely designed with COTS parts (Vilkomerson et al., 2008; Yonezawa et al., 1989; Allen et al., 1978; Tang et al., 2014; Cannata et al., 2012). COTS parts include monolithic integrated circuits (IC), connectors, jacks, discrete electrical components (i.e., resistors, capacitors, inductors), etc. They are routed and connected on a planar substrate, often multi-layer, called a printed circuit board (PCB) to facilitate interconnections between the individual COTS parts.

WID size reduction with COTS parts can be accomplished in several ways: two-sided COTS mounting (e.g.,(Vilkomerson et al., 2008)), multilayer PCBs (e.g., (Rothfuss et al., 2016)), and highly integrated ICs (e.g., (Vilkomerson et al., 2008; Gill and Meindl, 1975; Rothfuss et al., 2016)). Two-sided PCBs allow COTS parts to be mounted on both sides of the PCB, thereby shortening interconnections. Multilayer PCBs can be used with two-sided mounting to increase the interconnection density by routing signals, power, and ground

within the planar PCB itself. Highly integrated ICs offer the greatest amount of function in the highest density footprint; radios, microcontrollers, voltage regulators, temperature sensors, etc. can all be integrated into a single silicon die (e.g., CC1110 by Texas Instruments, TX, used by Rothfuss et al. in MFF monitoring (Rothfuss et al., 2016)). Nearly all present-day COTS components used in products are available in a surface mount technology (SMT) package, which allows components to be directly mounted on the PCB surface, rather using legacy through-hole mounting. SMT devices are typically small and allow for high PCB component densities. These techniques are typically combined to reduce the device size. The work done by Rothfuss et al., Unadkat et al., and Gimbel et al. shows a CW WID device that achieved the smallest reported electronics volume by combining multilayer PCBs, highly integrated ICs, and SMT COTS parts (Unadkat et al., 2014; Gimbel et al., 2014; Unadkat et al., 2015; Rothfuss et al., 2016).

Advancements in monolithics

Despite the advantages of COTS parts, they ill-suited for chronic implantation, due to their large footprint, compared with ICs. Highly integrated circuits reduce a design's real-estate. By incorporating a large number of transistors and components on silicon, enormous space savings can be obtained compared with COTS and PCB implementations.

While completely integrating a WID's functions on a single silicon die may seem like the overwhelmingly obvious solution towards miniaturization, manufacturing costs can be a significant development barrier. Newer fabrication generations offer the greatest area- and power-savings and performance, but their cost can be prohibitively high. For example, a modern 65 nm mask

set (i.e., available since 2006) can cost nearly $3 Million, while a mask set for an older process, the 0.35 μm node (i.e., available in 1995), can cost greater than an order of magnitude less (Wilson and Ismail, 2006).

CW and PW Doppler designs are highly dependent on analog circuits. Digital circuits are better suited for complimentary metal-oxide-semiconductor (CMOS) processes and analog circuits are better suited for a bipolar process. However, according to Baker (Baker, 2011) more than 95% of all manufactured integrated circuits are fabricated in a CMOS process. Therefore, devices with analog circuitry, such as WIDs, will likely be manufactured in a CMOS, rather than bipolar process. The digital circuits benefit greatly with each new process generation; however, analog circuit feature sizes have remained relatively unchanged, which obviates the cost-savings per area benefit offered by newer and more expensive process generations. Additionally, the yield of analog circuits is considerably less than digital circuits. When a silicon die contains both analog and digital circuits, the yield becomes limited by the yield of the analog circuits on chip (Wilson and Ismail, 2006). Therefore, from a cost savings standpoint, it may be prudent for WID research to pursue legacy process generations, such as the 0.35 μm process.

Throughout the entire body of published WID devices and studies, few have investigated monolithic's usefulness in WID devices. In fact, no studies have produced a totally integrated WID; rather, most incorporate several ICs and some discrete components. The earliest mention of a monolithic integrated implantable Doppler flowmeter was in 1969 by Meindl et al. (Meindl et al., 1969), and then again in 1972 by DiPietro et al. (DiPietro and Meindl, 1972), followed by continued development on the micropower integrated cir-

cuits by Frescura and DiPietro in 1976 and 1977 (Frescura and Meindl, 1976; DiPietro and Meindl, 1977). Even without a total monolithic implementation, the space-savings afforded by using several ICs improved on prior WID implant size by a factor of 5 to 10 while consuming an order of magnitude less power (Di Pietro and Meindl, 1978). DiPietro's CW WID, reported in 1978 measured less than 36 cm^3. Another WID, a PW configuration, reported in 1975 by Gill (Gill and Meindl, 1975), measured 60 cm^3, and its integrated circuit design was detailed by Gill et al. in (Gill, 1975). Later on, a smaller and bidirectional PW WID was developed by Allen et al. which measured 3.8 x 2.8 x 0.8 cm (Allen et al., 1978). Present day WIDs continue to use the same multiple-IC and discrete component implementations, albeit with increased levels of integration with more functions to be integrated into the same IC package (Vilkomerson and Chilipka, 2004; Vilkomerson, 2008; Tang et al., 2014; Rothfuss et al., 2016).

External demodulation

Efforts to reduce implant volume have resulted in another minimization technique, where extracting Doppler baseband information takes place at a device external to the monitored subject. The high frequency flow signals are telemetered to an external device by modulating the carrier frequency of a wireless link (i.e., typically an inductive link). Despite size reduction being the goal, the inductive links used to implement this technique use large coils, which add bulk. The CW WID developed by Cathignol et al. amplified the transduced blood flow signal followed by telemetering it remotely (Cathignol et al., 1975). The telemetry coil was 4 cm x 4 cm, but no further details regarding size were reported by the authors. A CW WID device developed

by Tang et al. also used this technique (Tang et al., 2014); however, their device used two coils. One larger coil provided power to recharge a battery, and a smaller coil solely for telemetering data to an external device, where the blood flow information was demodulated. The device coils required 2.5 cm and the area of the two PCBs occupied 7 cm^2.

Yonezawa et al. also reported devices that performed the demodulation and processing externally (Yonezawa et al., 1989, 1992). The Doppler flow information modulates an FM transmitter radio signal, which is then received externally and then filtered, demodulated, etc. Gill and Meindl (Gill and Meindl, 1975) and Allen et al. (Allen et al., 1978) demonstrated a variation of this technique with their PW WIDs, by demodulating on the implanted device, but performing the sample/hold and filtering externally. Gill and Meindl's device occupied 60 cm^3, with 20 % of the volume contributed by the electronics. Allen et al.'s device measurements were described in Section "Advancements in monolithics". Additionally, a unique variation on this size minimization technique was implemented by Hartley and Cole (Hartley and Cole, 1974). Their PW WID device used an implanted 3 cm diameter coil that connected directly to the transducer. Thereby locating all electronics externally.

WID Miniaturization Summary

A summary of the miniaturization techniques used throughout the developments of WIDs, both CW and PW, are shown in Table b. From the table, it is noted that the size of WIDs have stayed the same as those developed in the late 1960s and 1970s. This can be explained by noticing that the studies since the turn of the century have focused on proof-of-concept development

of advanced techniques improving accuracy (see Section: "Mechanisms of Doppler Ultrasound and Accuracy"), advancements in transducers (see Section: "Diffraction Grating Transducers"), wireless power (see Section: "Alternative power sources & safety limitations"), etc.

It should also be mentioned that the power source plays a crucial role in the size of the implant. For example, in the design of the PW WID by Gill in 1975 (Gill and Meindl, 1975), only 20% of the entire 60 cm^3 implant is occupied by electronics; Gill suggests that implant volume can be greatly reduced by replacing the battery with an inductive power link. However, Gill's PW WID consumes multiple milliwatts of power, which is likely to exceed specific absorption rate (SAR) limits mandated by the FCC (Rabaey et al., 2011). Therefore, Gill's implant would need further size and power reductions to permit wireless powering, but even with wireless power-enabled WIDs, the reported wireless techniques for the WIDs (Tang et al., 2014) and similar devices (Tang et al., 2011) is still multiple centimeters in size. It should be mentioned that special attention towards minimization of wireless power links is currently a rich field of research (see Section: "Alternative power sources & safety limitations").

Future WID miniaturization efforts should focus on increased silicon integration (i.e, towards a system on a chip), which will lead to ultra-small devices for chronic implantation. Recent research into ultra-miniaturized implants has also pursued ultra-low power implementations, which can run on scavenged energy or small batteries. Ultra-low power integrated circuit designs have been reported for numerous biological implant devices (e.g., for ECG, EEG, cochlear implants, etc.) (Neihart and Harrison, 2005; Sarpeshkar

et al., 2005; Verma et al., 2010; Burke and Gleeson, 2000; Fay et al., 2009) in low-cost technology nodes (e.g., 0.5 μm, 0.8 μm, etc.). However, the WID has been absent in integrated circuit literature since the late 1970s. Since the 1970s, significant research into ultra-low power techniques (Sarpeshkar, 2010), and higher speed and smaller size transistors have surfaced, which have not been exploited for WID miniaturization.

Power Sources and Lifetime

The power source is an integral part of WID design and lifetime. Batteries are the major go-to source for power, but they are often bulky and their lifetime is limited. Transcutaneous wireless power offers an unlimited implant lifetime, but its appearance in WID literature is scarce. This section discusses power sources and alternative power sources, as well as, suggests future directions for power savings specific to WIDs.

Battery Power

Battery power is the most prevalent WID power source reported in literature. Reported WIDs employ various types of batteries, each with their own limiations and advantages. For example, the WID developed by DiPietro used a 1.35 V mercury cell (Di Pietro and Meindl, 1978). The advantage of the mercury battery is that it can maintain its rated voltage for years. However, due to the toxicity of the mercury contained within these cells, they can no longer be purchased in most countries, and are not suited for future WID designs. Pacemaker batteries can also be found in WIDs and offer an avenue for chronic implantation. Using pacemaker batteries, the implants developed by Vilkomerson (Vilkomerson and Chilipka, 2004) and Cannata (Cannata

et al., 2012) can operate up to ten and nine years, respectively. The model reported by Vilkomerson is bulky and largely dominates the WID implant size, making it ill-suited for chronic implantation. Smaller pacemaker batteries do not necessarily translate to reduced size for chronic implanation. For example, the smallest available pacemaker, the Micra^{TM}Transcatheter Pacing System, achieved its longevity by improving the implanted electronics power consumption by an order of magnitude (Roe, Online; accessed 2016-09-25).

The high energy density and current sourcing capacity of lithium batteries makes them particularly useful for power demanding applications requiring a small footprint, such as cell phones, laptops, and implantable medical devices. Another advantage of some popular lithium battery chemistries is their high terminal voltage over the discharge cycle, such as in the case of lithium-ion polymer batteries (i.e., 3.7 V). WIDs reported by Vilkomerson (Vilkomerson et al., 2008), Tang et al. (Tang et al., 2014), and Rothfuss et al. and Unadkat et al. and Gimbel at al. (Unadkat et al., 2014; Gimbel et al., 2014; Unadkat et al., 2015; Rothfuss et al., 2016) all make use of rechargeable lithium batteries. Lithium cell size and energy density are likely to continue fueling their popularity for future WID development.

Alternative power sources & safety limitations

Alternative sources of power are attractive because they offer an unlimited implant operational lifetime. Chronic implant studies requiring years of monitoring, such as in artificial grafts, can benefit greatly from alternative power sources. To date, there are many identified alternate sources of power (Chandrakasan et al., 2008; Denisov and Yeatman, 2010; Rabaey et al., 2011; Olivo et al., 2011), including thermoelectric, light, kinetic motion

harvesters (i.e., piezoelectrics, electromagnetic, and electrostatic), near-field wireless power, far-field wireless power, ultrasonic power, etc. However, it is the dominant source of power consumption and the WID environment that dictate which of these alternative power sources are suitable. Two common WID components dominating the power consumption are the wireless radio (i.e., for telemetry) and the ultrasonic transducer driver. Wireless radio power consumption can be duty cycled to consume a low average power (See Section: "Low power standby modes"), but typical instantaneous current draws are in the low milliampere range. As for the transducer drive power, the lowest power consumption reported to date is 500 μW by Vilkomerson and Chilipka (Vilkomerson and Chilipka, 2004). Therefore, of the available alternative power sources, only the highest energy densities (e.g., transcutaneous wireless near-field powering and ultrasonic powering) are suitable for providing unlimited implant operational lifetime at the requisite power demands in a small implant size.

Transcutaneous wireless powering (TWP) is a rich field of research (Rabaey et al., 2011; Zhang et al., 2009; Si et al., 2008; Zargham and Gulak, 2012; Jow and Ghovanloo, 2007; Poon et al., 2007; Kiani et al., 2011), which is beyond the scope of this review. Recently, Several important milestones in TWP have been reported which have garnered significant attention. Motivated by a need to reduce the size of bulky implanted antennas for TWP, Poon et al. discovered that an optimal excitation frequency exists, based on new analysis of electromagnetic interactions with the various tissues in the body (Poon et al., 2010), and mid-field powering, rather than far- or near-field offers the greatest power availability for deep-seated implants without exceeding SAR

limits (Cleveland et al., 1997). Historically, TWP antennas were bulky due to the relation that electromagnetic power loss in the body increases with increases in frequency (i.e., $\lambda \propto \frac{1}{f}$) (Akin et al., 1998; Liu et al., 2000; Sauer et al., 2005). The work by Poon et al. (Poon et al., 2010) analyzed the optimality of the TWP frequency from the perspective that an implant will lie beneath a heterogeneous stackup of tissues (i.e., skin, fat, muscle, etc.), depending on the application. It is the difference in electromagnetic properties (i.e., permittivity, conductivity, etc.) of different tissues in a specific stackup (i.e., layer order) that leads to the understanding that the implant location will dictate the optimal frequency. Typically, the optimal frequency for most WPT-enabled implants lies in the 100s of MHz. Another significant advantage of TWP in the near- and mid-fields is that a single antenna can be used to both power the implant and telemeter data. If an implanted antenna were to be dedicated to TWP, then a second antenna would be needed for a radio transmitter, which draws considerable power, to telemeter data, adding additional bulk to the implant. The same circuitry used in RFID tags to send data back towards the external antenna/system is used in near- and mid-field powered medical implants, which makes data communication readily integrable with monolithic circuits.

To date, only one study has demonstrated TWP for a WID (Tang et al. (Tang et al., 2014)). However, the reported WID also made use of an implanted battery, which was recharged through TWP. Additionally, one study developed a unique method to enable an unlimited lifetime for chronic implantation studies. This study, by Hartley and Cole (Hartley and Cole, 1974), coiled the ultrasonic probe's lead wires to form a coil, which could

be electromagnetically coupled to by an external transformer coil integrated with a Doppler blood flowmeter; therefore, no electronics were implanted, only a coil and the ultrasonic probe. The novel minimalist approach to wireless flow monitoring employed by Hartley and Cole appeared to achieve what others could not: minimizing foreign material and minimizing implant complexity. However, for unclear reasons, the body of published literature has progressed with implanted electronic blood flow meters rather than Hartley's implementation. Neither Tang et al. nor Hartley and Cole reported on the safety of their trancutaneous wireless powering implementation (i.e., SAR limits), which may limit adoption of their unique approaches to chronic implantation. Future WID studies using TWP cannot neglect tissue heating effects.

Over the past decade, research has demonstrated the viability of using deployed stents (i.e., for treating atherosclerosis) as the TWP antenna, thereby eliminating the concerns over antenna bulk. Many different solutions to chronically and wirelessly monitor restenosis without a battery. Early efforts by Takahata et al. in 2003 (Takahata et al., 2003) and 2006 (Takahata et al., 2006) used a custom micromachined stent that when deployed, formed a coil meant to resonate with the capacitance of a capacitive pressure sensor; changes in intraluminal pressure ($\propto$ flow rate) shows a shift in the resonant frequency. Another pressure sensitive device, developed by DeHennis et al. (DeHennis and Wise, 2006), incorporated an integrated circuit along with its pressure sensor, but used a flexible spiral TWP antenna, rather than a stent, to fit within a vessel. DeHennis et al. recognized that maximizing the implanted antenna area would maximize coupling with the external an-

tenna, and suggested that the stent frame would satisfy this purpose. It was not until 2009, by Chow et al. (Chow et al., 2009), that the optimal frequency of the deployed stent in its environment was investigated, finding that 2.4 GHz performed best for cardiovascular stents in the chest. Chow et al. later demonstrated an intraluminal pressure monitor using the stent for the telemetry link, and secondary 3.7 GHz antenna for TWP (Chow et al., 2010). Between 2011 and 2012, Occhiuizzi et al. demonstrated a restenosis monitor by investigating changes in backscattered power due to dielectric property changes of the different atherosclerotic plaques (Occhiuzzi et al., 2011, 2012). However, it wasn't until 2012 that the first optimal TWP link using only a stent (i.e., no additional antennas for communicating or powering) was investigated by Keikhosravy et al. (Keikhosravy et al., 2012), who also considered the SAR effects of such an implementation in the chest. Keikhosravy et al. demonstrated the TWP stent-only power harvesting and communication system at 2.4 GHz using a custom designed ultra-low power integrated circuit (Keikhosravy et al., 2014). Keikhosravy's work shows the most promise when considering outfitting the stent antenna with Doppler blood flow transducers for flow monitoring. However, the power consumption for Doppler blood flow monitors remains significantly higher than the capacitive pressure sensor restenosis monitors (e.g., DeHennis et al. $-$ 340μW). Therefore, applications where a lower operating frequency can be used (i.e., to minimize power lost in tissue), such as for PAD in the lower limbs which uses larger stents than those in the chest, stands to increase the available power for the implant.

While TWP is the preferred power transfer scheme at short distances (i.e., 1 cm), it performs poorly for deeply seated implants. At deep implants depths

(i.e., 10 cm), ultrasonic power transfer shows greater efficiency (Denisov and Yeatman, 2010). This makes ultrasonic powering a better choice for WIDs used for monitoring applications such as coronary bypass grafts and buried free flaps, which are only accessible by current battery-powered WIDs and the wired implantable Doppler, and lay at distances beyond the reach of other popular blood flow monitoring techniques such as Laser Doppler or NIRS. The European Ultrasponder Project has been a recent effort in power delivery and wireless communication using ultrasound rather than electromagnetic waves (Mazzilli et al., 2010). The project focuses on milliwatt power delivery at depths of $10-20$ cm (Cotté et al., 2012; Mazzilli et al., 2014) via Radziemski and Makin (Radziemski and Makin, 2016). A major advantage of ultrasonic powering and communicating compared with TWP is its invariance to electromagnetic radiation, which eliminates hazardous electromagnetic interference with medical devices such as pacemakers (Van Der Togt et al., 2008).

A practical issue with ultrasonic powering for WIDs is large acoustic fields in proximity to the ultrasonic piezoelectric transducers used to sense Doppler blood flow signals. This scenario is tantamount to the same problem in mobile communication systems where where nearby strong interfering signals severly impact communication channels (Razavi, 1996). Sufficient frequency selectivity of front-end electronics and the Doppler-sensing transducers would be necessary in order to reject the interference and in order to combine the benefits of ultrasonic powering with Doppler blood flow monitors. A potential solution to using ultrasonic powering with WIDs is to enable the ultrasonic link to charge an energy storage element, such as a battery or supercapacitor.

Then, when blood flow data is to be collected, the ultrasonic link is disabled. This method was utilized by Tang et al. to electromagnetically wirelessly power a WID (Tang et al., 2014). A disadvantage to this technique is that continuous monitoring is no longer possible, which abandons the continuous monitoring tenet of the ideal blood flow monitor described by Smit et al. (Smit et al., 2010).

Powering an implantable device, or recharging a battery on the device, is not without limit. The transmission of energy through tissue results in unwanted heating. For electromagnetic TWP, the heating is caused by absorption (Bernardi et al., 2000), but for the ultrasonic powering case, the heating is caused by both absorption and cavitation (Dalecki, 2004). Regulatory limits on the maximum permissible rise in temperature effectively limit the amount of power that can be transmitted through tissue to a power harvesting implant. As transmission efficiency decreases (i.e., due to the electromagnetic (Gabriel et al., 1996) and acoustic attenuation properties of tissues (Culjat et al., 2010)), less power is available for the implant, necessitating power efficient electronics topologies or bulky storage elements such as batteries. For ultrasonic power delivery, limitations for the continuous powering case are more applicable (i.e., rather than pulsed excitation) for wireless implantable Doppler devices, in particular if the implant foregos an implantable battery to reduce bulk, and if the device is to be a truly continuous monitor (i.e., not "approximately continuous" as discussed in Section b for ideal monitors). However, according to Radziemski and Makin's 2016 review of continuous ultrasonic power delivery to charge a battery, the body of literature regarding its safety is limited (Radziemski and Makin, 2016).

Radziemski and Makin demonstrated safe power deliveries of 600 mW and 50 mW to implanted batteries at 10−15 mm and 50 mm, respectively, over a total of 10.5 hours during a five-week period. The implanted receiver transducer was circular and 25 mm in diameter and the operational frequency was 1 MHz. For electromagnetic TWP, the SAR limitations are well-known. For 1 gram of tissue, the average power cannot exceed 1.6 W/kg, while the average power in 10 grams of tissue cannot exceed 2 W/kg over 6 minutes (Kiourti et al., 2011). Recent work in the field of TWP, by Poon et al. (Poon et al., 2010), has demonstrated continuous safe power delivery in the milliwatt range for depths of several centimeters using a millimeter-sized receiver at about 1 GHz. Comparing the power delivery and ultrasound, ultrasound power delivery systems typically operate in the low-MHz due to a compromise for penetration and tissue heating (Denisov and Yeatman, 2010; Cotté et al., 2012). Whereas, the TWP demonstrated by Poon et al. operated at a carrier frequency three orders of magnitude greater − about 1 GHz. Not only does the smaller wavelength permit significant miniaturization, but a major benefit of a higher carrier frequency is that it can support higher data rates.

Other Approaches to power savings

Throughout WID literature, there have been several alternative approaches towards minimizing power consumption and maximizing implant lifetime that have proved successful.

Ultrasonic Frequency and Blood Backscattering

As reported early on in WID history by Gill and Meindl (Gill and Meindl, 1973), ultrasonic operational frequency is a critical system design specification. The majority of WID devices reported in literature operate in the low MHz range (i.e., <10 MHz). Vilkomerson described the benefits of increasing the ultrasonic frequency (Vilkomerson and Chilipka, 2004; Vilkomerson et al., 2008; Cannata et al., 2012), which include greater signal-to-noise ratios for a given power drive for the transmitting transducer. Vilkomerson's early reported WIDs were a CW configuration operating at 20 MHz. Later reports by the same author demonstrated 30 MHz and 40 MHz variations of the same WID.

Physical and biological mechanisms in an application environment affect selection of ultrasonic frequency. With direct access to a vessel, the ultrasonic wave travels through and impinges on the vessel wall and the blood within the vessel lumen. An optimal frequency can be established by accounting for the attenuation and scattering properties of the vessel wall and blood, which are functions of frequency. The goal is to minimize attenuation from the vessel wall and maximize backscattered energy from the blood. Hoskins established equations to predict these properties gathered from available literature (Hoskins, 2007). Hoskins' review shows that 20 MHz is a good trade-off between attenuation and backscatter. Blood backscattering holds a nearly f^4 dependency, which indicates Rayleigh scattering. Noteworthy devices that operate at 20 MHz are the gold-standard Cook-Swartz wire Doppler and several reported WIDs (Vilkomerson and Chilipka, 2004; Vilkomerson et al., 2008; Unadkat et al., 2014; Gimbel et al., 2014; Unadkat et al., 2015;

Rothfuss et al., 2016). As an example, using Hoskins' review, for the same transducer drive power, over 22 dB more backscattered power is available for these 20 MHz implementations compared with the 6 MHz CW WID by DiPietro (Di Pietro and Meindl, 1978). Therefore, attention to ultrasonic frequency in WID design is imperative to achieve high signal-to-noise ratio for a given drive power.

Low power standby modes

Continuous monitoring with chronically implanted WIDs, employing a battery, will render the device's power source depleted quickly. Duty cycling the battery usage is a convenient way to increase implant lifetime when the application can tolerate intermittent monitoring. In 2008, Vilkomerson et al. developed a CW WID capable of a 35 year implant lifetime with one measurement per day or an eight year lifetime with eight measurements per day (Vilkomerson et al., 2008). A study by Cannata et al. in 2012, using nearly the same device from Vilkomerson et al.'s 2008 study, provides a nine year lifetime with four measurements per day (Cannata et al., 2012). By duty cycling the battery usage, power draw remains in the micro- or nanowatt levels when the device isn't taking a measurement. This is accomplished through the use of electronics capable of powering themselves into a low-power mode (i.e., often called a sleep mode).

Low-power modes are a common feature in many electronic devices. Early WID devices were outfitted with an RF switch (Gill et al., 1976; Di Pietro and Meindl, 1978), which allowed the totally implanted WID to be wirelessly activated for when a measurement was desired. Before the advent of highly integrated microcontrollers and radios, WID research implemented custom

integrated circuit RF switch designs using a separate antenna than the main telemetry antenna. Recent WIDs reported by Vilkomerson et al. (Vilkomerson et al., 2008), Cannata et al. (Cannata et al., 2012), and Rothfuss et al. (Rothfuss et al., 2016) and Unadkat et al. (Unadkat et al., 2014, 2015) and Gimbel et al. (Gimbel et al., 2014), use highly integrated radios and radio/microcontroller systems on a chip which can achieve nanoampere current draws in sleep mode, all while incorporating the switch using the same antenna used for telemetry. For example, Rothfuss et al.'s reported WID could only stay on for about 3 hours and 20 minutes continuously. However, when using a sleep mode, their device achieved over three weeks of standby time by waking up every 33 seconds to check for an incoming wake up signal (Rothfuss et al., 2016).

Diffraction Grating Transducers

Previous WIDs reported that their piezoelectric transducer drive power was in the tens of milliwatts or more (Gill and Meindl, 1975; Allen et al., 1977; Cannata et al., 2012). With maximizing implant lifetime being such a critical concern in WID research, it is interesting to note that little attention is given to minimizing transducer power consumption. To date, the lowest power required to drive a transducer for accurate direct-contact blood flow monitoring is 500 μW, reported by Vilkomerson for a double-beam diffraction grating transducer (DGT) (Vilkomerson and Chilipka, 2004). Vilkomerson's research with DGTs has produced low power and angle-independent accurate blood flow measurements (Vilkomerson et al., 1994, 1997, 1998; Vilkomerson, 2008).

Outlook and Concluding Remarks

Totally implantable wireless ultrasonic blood flow monitors are a useful technology for providing accurate and chronic monitoring of blood flow, such as in free flaps, artificial grafts, and freely behaving physiological studies. This paper summarizes both early and recent WID advances that have lead to more accurate, smaller, and longer lasting devices. While a desired accuracy can be tailored for the application, the size and implant lifetime of devices throughout literature is insufficient to meet the demands for low foreign body response and chronic monitoring, despite the continued advancement of technology according to Moore's law. The following provides a brief summary of findings and recommendations to achieve a desired accuracy, size, and implant lifetime for the next generation of WIDs:

- Accurate WIDs have been in existence for many years. Little has changed since the development of PW Doppler devices, which provide superior accuracy over CW Doppler configurations. However, assessing the application needs may preclude the need for a PW configuration. The PW configuration is more complex and generally more power demanding than the CW configuration, which can lead to a size and power savings for some applications, such as patency detection and areas of known flow and vascular dimensions. Another accuracy improvement can be obtained by incorporating the recently developed DGT. The DGT offers an angle-independent measurement, which eliminates a major source of error − assumed insonation angle when determining it is difficult or impractical. DGTs have been reported to consume very little power for their accuracy.

- WID miniaturization and implant lifetime are strongly related (i.e., battery capacity or implanted antenna size). While COTS components and PCBs are convenient for prototyping, reported WID devices employing these remain bulky and offer limited room for increasing implant lifetime. Integrated circuits have recently enabled ultra-small and ultra-low power implantable medical devices that can operate without batteries. Highly integrated WID devices have not been reported in literature, and this technology stands to usher in the smallest and least-power demanding devices.

- Implant lifetime needs to be maximized for chronic monitoring applications, such as wireless restenosis monitoring. Batteries are the most common source of power for WIDs, but they are limited in available power and/or recharge cycles. Incorporating energy scavenging technologies into WIDs can lead to batteryless devices with unlimited implant lifetimes. However, some sources of power, such as thermoelectric power or kinetic harvesting, do not offer a high enough energy density for current WID designs. Both TWP and ultrasonic power transfer offer solutions capable of delivering milliwatts of power safely to implants.

  In TWP systems, the far-field and most importantly, near-field powering offer high energy densities that have successfully powered other implanted devices in literature; however, their link range is often limited to a couple centimeters. Ultrasonic power delivery offers efficiency improvements at greater implant depths and immunity to electromagnetic interference; however, the piezoelectric transducers and front-end electronics in WIDs used to sense Doppler blood flow signals will likely

suffer from interference by the large transmitted acoustic fields for powering. A workaround could be to charge an energy storage element (e.g., battery or supercapacitor) with ultrasonic power first, then power the WID from the energy storage element with ultrasonic powering turned off. A disadvantage to this technique is that continuous monitoring would no longer be possible (i.e., for immediate detection of loss of flow). To the best of the authors' knowledge, ultrasonic powering of WIDs has yet to be investigated, and the use of ultrasonic powering of WID stands to extend WIDs to implant depths unattainable by TWP WIDs, which would be a valuable contribution to the field. For shallower implant depths, WIDs should pursue TWP as a future source of power to achieve chronic monitoring.

A barrier towards WID's adoption of TWP is that antenna size and link efficiency need to be optimized for each specific application site, which implies that no single TWP solution will be optimal for all implant sites. However, for the case of a chronically implanted wireless restenosis monitor, the stent itself serves as the antenna, obviating concerns about implanting a bulky antenna. The large implanted stents used in treating PAD stand to provide more power to an implant and should be pursued first when using Doppler blood flow sensors for chronic restensois monitoring. Ultimately, for any chronic implant, whether using ultrasonic powering or TWP, local heating of delicate tissues is a concern and devices must adhere to regulatory limitations, which impose power delivery maximums and increase the burden of efficient electronic design.

962 Akin T, Najafi K, Bradley RM. A wireless implantable multichannel digital
963 neural recording system for a micromachined sieve electrode. IEEE Journal
964 of Solid-State Circuits, 1998;33:109–118.

965 Allen HV, Anderson MF, Meindl JD. Direct calibration of a totally im-
966 plantable pulsed Doppler ultrasonic blood flowmeter. American Journal
967 of Physiology, 1977;232:537–544.

968 Allen HV, Knutti JW, Meindl JD. Integrated circuits for a bidirectional
969 implantable pulsed Doppler ultrasonic blood flowmeter. IEEE Journal of
970 Solid-State Circuits, 1978;13:853–863.

971 Arger P, Iyoob S. The Complete Guide to Vascular Ultrasound. LWW med-
972 ical book collection. Lippincott Williams & Wilkins, 2004.
973 URL https://books.google.com/books?id=L2WnFmR9oVwC

974 Axelsson M, Dang Q, Pitsillides K, Munns S, Hicks J, Kassab GS. A novel,
975 fully implantable, multichannel biotelemetry system for measurement of
976 blood flow, pressure, ECG, and temperature. Journal of Applied Physiol-
977 ogy, 2007;102:1220–1228.

978 Baker DW. Pulsed ultrasonic Doppler blood-flow sensing. IEEE Transactions
979 on Sonics and Ultrasonics, 1970;17:170–184.

980 Baker RJ. CMOS: circuit design, layout, and simulation. Vol. 18. John Wiley
981 and Sons, Hoboken, New Jersey, 2011.

982 Bernardi P, Cavagnaro M, Pisa S, Piuzzi E. Specific absorption rate and tem-
983 perature increases in the head of a cellular-phone user. IEEE transactions
984 on microwave theory and techniques, 2000;48:1118–1126.

985 Boote EJ. Aapm/rsna physics tutorial for residents: Topics in us: Doppler
986 us techniques: Concepts of blood flow detection and flow dynamics 1.
987 Radiographics, 2003;23:1315–1327.

988 Brody WR, Meindl JD. Theoretical analysis of the CW Doppler ultrasonic
989 flowmeter. IEEE Transactions on Biomedical Engineering, 1974;BME-
990 21:183–192.

991 Brunner E. How ultrasound system considerations influence front-end com-
992 ponent choice. Analog Dialogue, 2002;36:1–4.

993 Burke MJ, Gleeson DT. A micropower dry-electrode ECG preamplifier. IEEE
994 Transactions on Biomedical Engineering, 2000;47:155–162.

995 Cannata JM, Chilipka T, Yang HC, Han S, Ham SW, Rowe VL, Weaver
996 FA, Shung KK, Vilkomerson D. Development of a flexible implantable
997 sensor for postoperative monitoring of blood flow. Journal of Ultrasound
998 in Medicine, 2012;31:1795–1802.

999 Cathignol D, Chapelon JY, Jossinet J, Lavandier B, Fourcade C. Detailed
1000 description of an implantable directional Doppler flowmeter. Biotelemetry,
1001 1975;3:117–128.

1002 Chandrakasan AP, Verma N, Daly DC. Ultralow-power electronics for
1003 biomedical applications. Annual Review of Biomedical Engineering,
1004 2008;10:247–274.

1005 Chen K, Mardini S, Chuang DC, Lin C, Cheng M, Lin Y, Huang W, Tsao C,
1006 Wei F. Timing of presentation of the first signs of vascular compromise dic-

tates the salvage outcome of free flap transfers. Plastic and Reconstructive Surgery, 2007;120:187–195.

Cho BC, Shin DP, Byun JS, Park JW, Baik BS. Monitoring flap for buried free tissue transfer: its importance and reliability. Plastic and Reconstructive Surgery, 2002;110:1249–1258.

Chow EY, Chlebowski AL, Chakraborty S, Chappell WJ, Irazoqui PP. Fully wireless implantable cardiovascular pressure monitor integrated with a medical stent. IEEE Transactions on Biomedical Engineering, 2010;57:1487–1496.

Chow EY, Ouyang Y, Beier B, Chappell WJ, Irazoqui PP. Evaluation of cardiovascular stents as antennas for implantable wireless applications. IEEE Transactions on Microwave Theory and Techniques, 2009;57:2523–2532.

Chowdary RP, Campbell SP, Rosenberg M, Hugo NE. Dermofluorometric prediction of flap survival. Annals of plastic surgery, 1987;19:154–157.

Cleveland RF, Sylvar DM, Ulcek JL. Evaluating compliance with FCC guidelines for human exposure to radiofrequency electromagnetic fields. Standards Development Branch, Allocations and Standards Division, Office of Engineering and Technology, Federal Communications Commission, 1997.

Cotté B, Lafon C, Dehollain C, Chapelon JY. Theoretical study for safe and efficient energy transfer to deeply implanted devices using ultrasound. IEEE transactions on ultrasonics, ferroelectrics, and frequency control, 2012;59:1674–1685.

Culjat MO, Goldenberg D, Tewari P, Singh RS. A review of tissue substitutes for ultrasound imaging. Ultrasound in medicine & biology, 2010;36:861–873.

Dalecki D. Mechanical bioeffects of ultrasound. Annual Review of Biomedical Engineering, 2004;6:229–248.

D'Ancona G, Karamanoukian H, Salerno T, Schmid S, Bergsland J. Flow measurement in coronary surgery. In: The Heart Surgery Forum. Vol. 2, 1999. pp. 121–4.

DeHennis AD, Wise KD. A fully integrated multisite pressure sensor for wireless arterial flow characterization. Journal of Microelectromechanical Systems, 2006;15:678–685.

Denisov A, Yeatman E. Ultrasonic vs. inductive power delivery for miniature biomedical implants. In: 2010 International Conference on Body Sensor Networks. IEEE, 2010. pp. 84–89.

Di Pietro DM, Meindl JD. Optimal system design for an implantable CW Doppler ultrasonic flowmeter. IEEE Transactions on Biomedical Engineering, 1978;25:255–264.

DiPietro D, Meindl J. An implantable blood flowmeter using monolithic integrated circuits. In: 1972 IEEE International Solid-State Circuits Conference: Digest of Technical Papers. Vol. 15. IEEE, 1972. pp. 184–185.

DiPietro DM, Meindl JD. Integrated circuits for an implantable CW Doppler ultrasonic flowmeter. IEEE Journal of Solid-State Circuits, 1977;12:573–576.

1052 Disa JJ, Cordeiro PG, Hidalgo DA. Efficacy of conventional monitoring tech-
1053 niques in free tissue transfer: an 11-year experience in 750 consecutive
1054 cases. Plastic and Reconstructive Surgery, 1999;104:97–101.

1055 Fay L, Misra V, Sarpeshkar R. A micropower electrocardiogram amplifier.
1056 IEEE Transactions on Biomedical Circuits and Systems, 2009;3:312–320.

1057 Franklin DE, Watson NW, Pierson KE, Van Citters RL. Technique for radio
1058 telemetry of blood-flow velocity from unrestrained animals. The American
1059 Journal of Medical Electronics, 1965;5:24–28.

1060 Franklin DL. Blood velocity telemetered from untethered animals. Nature,
1061 1964;203:528–530.

1062 Franklin DL, Schlegel W, Rushmer RF. Blood flow measured by Doppler
1063 frequency shift of back-scattered ultrasound. Science, 1961;134:564–565.

1064 Frescura BL, Meindl JD. Micropower integrated circuits for an implantable
1065 bidirectional blood flowmeter. IEEE Journal of Solid-State Circuits,
1066 1976;11:817–825.

1067 Furnas H, Rosen JM. Monitoring in microvascular surgery. Annals of plastic
1068 surgery, 1991;26:265–272.

1069 Gabriel S, Lau R, Gabriel C. The dielectric properties of biological tissues: II.
1070 measurements in the frequency range 10 Hz to 20 GHz. Physics in medicine
1071 and biology, 1996;41:2251.

1072 Gill R, Meindl JD. Low power integrated circuits for an implantable pulsed

Doppler ultrasonic blood flowmeter. IEEE Journal of Solid-State Circuits, 1975;10:464–471.

Gill RW. An implantable pulsed Doppler ultrasonic blood flowmeter using custom integrated circuits, 1975.

Gill RW. Measurement of blood flow by ultrasound: accuracy and sources of error. Ultrasound in Medicine and Biology, 1985;11:625–641.

Gill RW, Hottinger CF, Meindl JD. Doppler instrumentation for measuring blood velocity and flow. In: Cardiovascular Imaging and Image Processing: Theory and Practice. International Society for Optics and Photonics, 1976. pp. 53–64.

Gill RW, Meindl JD. Optimal system design of the pulsed Doppler ultrasonic blood flowmeter. In: 1973 Ultrasonics Symposium, 1973. pp. 88–93.

Gill RW, Meindl JD, Haase WC. An implantable pulsed Doppler ultrasonic flowmeter. In: 24th Proceedings of the annual Conference on Engineering in Medicine and Biology. Vol. 13, 1971. p. 268.

Gimbel ML, Rothfuss MA, Unadkat JV, Mickle MH, Sejdic E. Venous flow monitoring using an entirely implanted, wireless Doppler sensor. Plastic and Reconstructive Surgery, 2014;133:126.

Goodstein WA, Buncke Jr HJ. Patterns of vascular anastomoses vs. success of free groin flap transfers. Plastic and Reconstructive Surgery, 1979;64:37–40.

1094 Graham BH, Walton RL, Elings VB, Lewis FR. Surface quantification of in-
1095 jected fluorescein as a predictor of flap viability. Plastic and reconstructive
1096 surgery, 1983;71:826–831.

1097 Gräns A, Axelsson M, Pitsillides K, Olsson C, Höjesjö J, Kaufman RC,
1098 Cech Jr J. A fully implantable multi-channel biotelemetry system for mea-
1099 surement of blood flow and temperature: a first evaluation in the green
1100 sturgeon. Hydrobiologia, 2009;619:11–25.

1101 Guillemaud JP, Seikaly H, Cote D, Allen H, Harris JR. The implantable cook-
1102 swartz Doppler probe for postoperative monitoring in head and neck free
1103 flap reconstruction. Archives of Otolaryngology–Head and Neck Surgery,
1104 2008;134:729–734.

1105 Guo Z, Durand LG, Allard L, Cloutier G, Lee HC. Classification of lower
1106 limb arterial stenoses from doppler blood flow signal analysis with time-
1107 frequency representation and pattern recognition techniques. Ultrasound
1108 in medicine & biology, 1994;20:335–346.

1109 Gupta M. An economic analysis of implantable Doppler technology in head
1110 and neck reconstruction. Ph.D. thesis, Université d'Ottawa/University of
1111 Ottawa, 2012.

1112 Hartley CJ, Cole JS. An ultrasonic pulsed Doppler system for measuring
1113 blood flow in small vessels. Journal of Applied Physiology, 1974;37:626–
1114 629.

1115 Hong JP, Yim JH, Malzone G, Lee KJ, Dashti T, Suh HS. The thin gluteal

artery perforator free flap to resurface the posterior aspect of the leg and foot. Plastic and Reconstructive Surgery, 2014;133:1184–1191.

Hoskins PR. Physical properties of tissues relevant to arterial ultrasound imaging and blood velocity measurement. Ultrasound in Medicine and Biology, 2007;33:1527–1539.

Jow UM, Ghovanloo M. Design and optimization of printed spiral coils for efficient transcutaneous inductive power transmission. IEEE Transactions on Biomedical Circuits and Systems, 2007;1:193–202.

Kang MJ, Chung CH, Chang YJ, Kim KH. Reconstruction of the lower extremity using free flaps. Archives of Plastic Surgery, 2013;40:575–583.

Keikhosravy K, Kamalinejad P, Keikhosravy L, Zargaran-Yazd A, Takahata K, Mirabbasi S. A fully integrated telemonitoring system for diagnosing in-stent restenosis. In: 2014 IEEE Biomedical Circuits and Systems Conference. IEEE, 2014. pp. 392–395.

Keikhosravy K, Zargaran-Yazd A, Mirabbasi S. On the use of smart stents for monitoring in-stent restenosis. In: 2012 Annual International Conference of the IEEE Engineering in Medicine and Biology Society. IEEE, 2012. pp. 3231–3234.

Kempton SJ, Poore SO, Chen JT, Afifi AM. Free flap monitoring using an implantable anastomotic venous flow coupler: Analysis of 119 consecutive abdominal-based free flaps for breast reconstruction. Microsurgery, 2015;35:337–344.

1138 Kiani M, Jow UM, Ghovanloo M. Design and optimization of a 3-coil induc-
1139 tive link for efficient wireless power transmission. Biomedical Circuits and
1140 Systems, IEEE Transactions on, 2011;5:579–591.

1141 Kiourti A, Christopoulou M, Nikita KS. Performance of a novel minia-
1142 ture antenna implanted in the human head for wireless biotelemetry. In:
1143 2011 IEEE International Symposium on Antennas and Propagation. IEEE,
1144 2011. pp. 392–395.

1145 Kong W, Rollins DL, Ideker RE, Smith WM. Design and initial evaluation of
1146 an implantable sonomicrometer and CW Doppler flowmeter for simultane-
1147 ous recordings with a multichannel telemetry system. IEEE Transactions
1148 on Biomedical Engineering, 2005;52:1365–1367.

1149 Liu W, Vichienchom K, Clements M, DeMarco SC, Hughes C, McGucken E,
1150 Humayun MS, De Juan E, Weiland JD, Greenberg R. A neuro-stimulus
1151 chip with telemetry unit for retinal prosthetic device. IEEE Journal of
1152 Solid-State Circuits, 2000;35:1487–1497.

1153 Liu Y, Zhao Y, Huang J, Wu Y, Jiang L, Wang G, Li W, Chen X, Shi R.
1154 Analysis of 13 cases of venous compromise in 178 radial forearm free flaps
1155 for intraoral reconstruction. International Journal of Oral and Maxillofacial
1156 Surgery, 2012;41:448–452.

1157 Lohman RF, Langevin CJ, Bozkurt M, Kundu N, Djohan R. A prospective
1158 analysis of free flap monitoring techniques: physical examination, external
1159 Doppler, implantable Doppler, and tissue oximetry. Journal of Reconstruc-
1160 tive Microsurgery, 2013;29:051–056.

1161 Mazzilli F, Lafon C, Dehollain C. A 10.5 cm ultrasound link for deep im-
1162 planted medical devices. IEEE transactions on biomedical circuits and
1163 systems, 2014;8:738–750.

1164 Mazzilli F, Peisino M, Mitouassiwou R, Cotté B, Thoppay P, Lafon C,
1165 Favre P, Meurville E, Dehollain C. *In-vitro* platform to study ultrasound
1166 as source for wireless energy transfer and communication for implanted
1167 medical devices. In: 2010 Annual International Conference of the IEEE
1168 Engineering in Medicine and Biology. IEEE, 2010. pp. 3751–3754.

1169 McDermott MM, Guralnik JM, Ferrucci L, Tian L, Liu K, Liao Y, Green
1170 D, Sufit R, Hoff F, Nishida T, et al. Asymptomatic peripheral arterial
1171 disease is associated with more adverse lower extremity characteristics than
1172 intermittent claudication. Circulation, 2008;117:2484–2491.

1173 McLeod FD, Anliker M. Multiple gate pulsed Doppler flowmeter. In: IEEE
1174 Transactions on sonics and ultrasonics. No. 3, 1971. p. 401.

1175 Meindl J. Implantable ultrasonic blood flowmeters. In: International Teleme-
1176 tering Conference Proceedings. International Foundation for Telemetering,
1177 1972.

1178 Meindl JD, McVittie JP, DiPietro DM. An implantable ultrasonic blood
1179 flowmeter utilizing monolithic integrated circuits. In: Proceedings of the
1180 8th International Conference on Engineering in Medical and Biological
1181 Engineering and the 22nd Annual Conference EMB. Chicago, Illinois, 1969.

1182 Morais JM, Papadimitrakopoulos F, Burgess DJ. Biomaterials/tissue inter-

actions: possible solutions to overcome foreign body response. The AAPS Journal, 2010;12:188–196.

Muradin GSR, Bosch JL, Stijnen T, Hunink MGM. Balloon dilation and stent implantation for treatment of femoropopliteal arterial disease: Meta-analysis. Radiology, 2001;221:137–145.

Neihart NM, Harrison RR. Micropower circuits for bidirectional wireless telemetry in neural recording applications. IEEE Transactions on Biomedical Engineering, 2005;52:1950–1959.

Nelson TR, Pretor DH. The Doppler signal: where does it come from and what does it mean? American Journal of Roentgenology, 1988;151:439–447.

O'Brien B, Morrison WA, Ishida H, MacLeod AM, Gilbert A. Free flap transfers with microvascular anastomoses. British Journal of Plastic Surgery, 1974;27:220–230.

Occhiuzzi C, Contri G, Marrocco G. RFID STENTag for passive vascular monitoring. In: Proceedings of the 5^{th} European Conference on Antennas and Propagation. IEEE, 2011. pp. 3476–3478.

Occhiuzzi C, Contri G, Marrocco G. Design of implanted RFID tags for passive sensing of human body: the STENTag. IEEE Transactions on Antennas and Propagation, 2012;60:3146–3154.

Oliver DW, Whitaker IS, Giele H, Critchley P, Cassell O. The cook–swartz venous Doppler probe for the post-operative monitoring of free tissue trans-

fers in the United Kingdom: a preliminary report. British Journal of Plastic Surgery, 2005;58:366–370.

Olivo J, Carrara S, De Micheli G. Energy harvesting and remote powering for implantable biosensors. IEEE Sensors Journal, 2011;11:1573–1586.

Paydar KZ, Hansen SL, Chang DS, Hoffman WY, Leon P. Implantable venous Doppler monitoring in head and neck free flap reconstruction increases the salvage rate. Plastic and Reconstructive Surgery, 2010;125:1129–1134.

Peronneau PA, Leger F. Doppler ultrasonic pulsed blood flowmeter. In: Proc. 8th Int. Conf. Med. Biol. Eng, 1969. pp. 10–11.

Poon AS, O'Driscoll S, Meng TH. Optimal operating frequency in wireless power transmission for implantable devices. In: 29th Annual International Conference of the IEEE Engineering in Medicine and Biology Society. IEEE, 2007. pp. 5673–5678.

Poon AS, O'Driscoll S, Meng TH. Optimal frequency for wireless power transmission into dispersive tissue. IEEE Transactions on Antennas and Propagation, 2010;58:1739–1750.

Pryor SG, Moore EJ, Kasperbauer JL. Implantable Doppler flow system: Experience with 24 microvascular free-flap operations. Otolaryngology-Head and Neck Surgery, 2006;135:714–718.

Rabaey JM, Mark M, Chen D, Sutardja C, Tang C, Gowda S, Wagner M, Werthimer D. Powering and communicating with mm-size implants. In:

2011 Design, Automation and Test in Europe Conference and Exhibition, 2011. pp. 1–6.

Radermacher J, Chavan A, Bleck J, Vitzthum A, Stoess B, Gebel MJ, Galanski M, Koch KM, Haller H. Use of Doppler ultrasonography to predict the outcome of therapy for renal-artery stenosis. New England Journal of Medicine, 2001;344:410–417.

Radziemski L, Makin IRS. In vivo demonstration of ultrasound power delivery to charge implanted medical devices via acute and survival porcine studies. Ultrasonics, 2016;64:1–9.

Razavi B. Challenges in portable rf transceiver design. IEEE Circuits and Devices Magazine, 1996;12:12–25.

Roe D. Secrets of Micra: How medtronic reinvented the pacemaker. http://www.meddeviceonline.com/doc/secrets-of-micra-0001, Online; accessed 2016-09-25.

Rosenberg JJ, Fornage BD, Chevray PM. Monitoring buried free flaps: limitations of the implantable Doppler and use of color duplex sonography as a confirmatory test. Plastic and Reconstructive Surgery, 2006;118:109–113.

Rothfuss MA, Franconi NG, Unadkat JV, Gimbel ML, Star A, Mickle MH, Sejdić E. A system for simple real-time anastomotic failure detection and wireless blood flow monitoring in the lower limbs. IEEE Journal of Translational Engineering in Health and Medicine, 2016. Accepted.

Rozen WM, Ang GG, McDonald AH, Sivarajah G, Rahdon R, Acosta R, Thomas DJ. Sutured attachment of the implantable Doppler probe cuff for

large or complex pedicles in free tissue transfer. Journal of Reconstructive Microsurgery, 2011;27:99–102.

Sarpeshkar R. Ultra low power bioelectronics: fundamentals, biomedical applications, and bio-inspired systems. Cambridge University Press, 2010.

Sarpeshkar R, Salthouse C, Sit JJ, Baker MW, Zhak SM, Lu TT, Turicchia L, Balster S. An ultra-low-power programmable analog bionic ear processor. IEEE Transactions on Biomedical Engineering, 2005;52:711–727.

Sauer C, Stanacevic M, Cauwenberghs G, Thakor N. Power harvesting and telemetry in cmos for implanted devices. IEEE Transactions on Circuits and Systems I: Regular Papers, 2005;52:2605–2613.

Schrey AR, Kinnunen IA, Grénman RA, Minn HR, Aitasalo KM. Monitoring microvascular free flaps with tissue oxygen measurement and PET. European Archives of Oto-Rhino-Laryngology, 2008;265:105–113.

Selvin E, Erlinger TP. Prevalence of and risk factors for peripheral arterial disease in the United States results from the national health and nutrition examination survey, 1999–2000. Circulation, 2004;110:738–743.

Service IR. Yearly average currency exchange rates translating foreign currency into U.S. dollars. https://www.irs.gov/individuals/international-taxpayers/yearly-average-currency-exchange-rates, 2016. [Online; accessed 06-June-2016].

Shung KK. Diagnostic ultrasound: Imaging and blood flow measurements. CRC press, Boca Raton, FL, 2005.

Si P, Hu AP, Malpas S, Budgett D. A frequency control method for regulating wireless power to implantable devices. IEEE Transactions on Biomedical Circuits and Systems, 2008;2:22–29.

Smit JM, Zeebregts CJ, Acosta R, Werker PM. Advancements in free flap monitoring in the last decade: a critical review. Plastic and reconstructive surgery, 2010;125:177–185.

Swartz WM, Jones NF, Cherup L, Klein A. Direct monitoring of microvascular anastomoses with the 20-mhz ultrasonic Doppler probe: An experimental and clinical study. Plastic and Reconstructive Surgery, 1988;81:149–158.

Takahata K, DeHennis A, Wise KD, Gianchandani YB. Stentenna: a micromachined antenna stent for wireless monitoring of implantable microsensors. In: Proceedings of the 25^{th} Annual International Conference of the IEEE Engineering in Medicine and Biology Society. Vol. 4. IEEE, 2003. pp. 3360–3363.

Takahata K, Gianchandani YB, Wise KD. Micromachined antenna stents and cuffs for monitoring intraluminal pressure and flow. Journal of Microelectromechanical Systems, 2006;15:1289–1298.

Tang SC, Jolesz FA, Clement GT. A wireless batteryless deep-seated implantable ultrasonic pulser-receiver powered by magnetic coupling. IEEE Transactions on Ultrasonics, Ferroelectrics and Frequency Control, 2011;58:1211–1221.

Tang SC, Vilkomerson D, Chilipka T. Magnetically-powered implantable

Doppler blood flow meter. In: 2014 IEEE International Ultrasonics Symposium (IUS). IEEE, 2014. pp. 1622–1625.

Unadkat J, Rothfuss M, Mickle MH, Sejdic E, Gimbel M. Entirely implanted wireless Doppler sensor for monitoring venous flow. Plastic and Reconstructive surgery, 2014;134:57–58.

Unadkat JV, Rothfuss M, Mickle MH, Sejdic E, Gimbel ML. The development of a wireless implantable blood flow monitor. Plastic and reconstructive surgery, 2015;136:199–203.

Upile T, Jerjes W, El Maaytah M, Hopper C, Searle A, Wright A. Direct microvascular monitoring of a free autologous jejunal flap using microendoscopy: a case report. BMC Ear, Nose and Throat Disorders, 2006;6:14–19.

Van Der Togt R, van Lieshout EJ, Hensbroek R, Beinat E, Binnekade J, Bakker P. Electromagnetic interference from radio frequency identification inducing potentially hazardous incidents in critical care medical equipment. Journal of the American Medical Association, 2008;299:2884–2890.

Verma N, Shoeb A, Bohorquez J, Dawson J, Guttag J, Chandrakasan AP. A micro-power EEG acquisition soc with integrated feature extraction processor for a chronic seizure detection system. IEEE Journal of Solid-State Circuits, 2010;45:804–816.

Vilkomerson D. Double-beam diffraction-grating transducers for improved blood flow measurement. In: 2008 IEEE Ultrasonics Symposium, 2008. pp. 1064–1067.

Vilkomerson D, Chilipka T. Implantable doppler system for self-monitoring vascular grafts. In: 2004 IEEE Ultrasonics Symposium. Vol. 1, 2004. pp. 461–465 Vol.1.

Vilkomerson D, Chilipka T, Bogan J, Blebea J, Choudry R, Wang J, Salvatore M, Rotella V, Soundararajan K. Implantable ultrasound devices. In: Medical Imaging. International Society for Optics and Photonics, 2008. pp. 69200C–69200C.

Vilkomerson D, Lyons D, Chilipka T. Diffractive transducers for angle-independent velocity measurements. In: Proc. of the 1994 IEEE Ultrasonics Symposium, 1994. Vol. 3, 1994. pp. 1677–1682.

Vilkomerson D, Lyons D, Chilipka T, Delamere M, Lopath P, Palanchon P, Shung K. Clinical blood flow measurements using diffraction-grating transducers. In: Proc. of the 1998 IEEE Ultrasonics Symposium. Vol. 2, 1998. pp. 1501–1508.

Vilkomerson D, Lyons D, Chilipka T, Lopath P, Shung KK. Diffraction-grating transducers. In: Proc. of the 1997 IEEE Ultrasonics Symposium. Vol. 2, 1997. pp. 1691–1696.

Webster JG. Measurement of flow and volume of blood. Medical instrumentation: application and design, 1998;2.

Wells PNT. A range-gated ultrasonic Doppler system. Medical and Biological Engineering, 1969;7:641–652.

Wilson J, Ismail M. Rfic design for first-pass silicon success. In: Radio Design in Nanometer Technologies. Springer, 2006. pp. 287–314.

Wu C, Lin P, Chew K, Kuo Y. Free tissue transfers in head and neck reconstruction: complications, outcomes and strategies for management of flap failure: analysis of 2019 flaps in single institute. Microsurgery, 2013;34:339–344.

Yonezawa Y, Caldwell WM, Schadt JC, Hahn AW. A miniaturized ultrasonic flowmeter and telemetry transmitter for chronic animal blood flow measurements. Biomedical Sciences Instrumentation, 1989;25:107.

Yonezawa Y, Nakayama T, Ninomiya I, Caldwell WM. Radio telemetry directional ultrasonic blood flowmeter for use with unrestrained animals. Medical and Biological Engineering and Computing, 1992;30:659–665.

Yu P, Chang DW, Miller MJ, Reece G, Robb GL. Analysis of 49 cases of flap compromise in 1310 free flaps for head and neck reconstruction. Head and Neck, 2009;31:45–51.

Zargham M, Gulak PG. Maximum achievable efficiency in near-field coupled power-transfer systems. IEEE Transactions on Biomedical Circuits and Systems, 2012;6:228–245.

Zhang F, Liu X, Hackworth SA, Sclabassi RJ, Sun M. *In vitro* and *in vivo* studies on wireless powering of medical sensors and implantable devices. In: Life Science Systems and Applications Workshop. IEEE, 2009. pp. 84–87.

Zhang T, Dyalram-Silverberg D, Bui T, Caccamese J, Lubek J. Analysis of an implantable venous anastomotic flow coupler: experience in head and

neck free flap reconstruction. International journal of oral and maxillofacial surgery, 2012;41:751–755.

Zhou W, He M, Liao Y, Yao Z. Reconstructing a complex central facial defect with a multiple-folding radial forearm flap. Journal of Oral and Maxillofacial Surgery: Official Journal of the American Association of Oral and Maxillofacial Surgeons, 2014;72:836–e1.

Figure Captions

Figure 1: System-level block diagram of the nondirectional Pulsed Wave Doppler flowmeter. Adapted from (Shung, 2005; Boote, 2003; Brunner, 2002).

Figure 2: System-level block diagram of the nondirectional Continuous Wave Doppler flowmeter.

Tables

Table 1: Summary of blood flow monitoring modalities and their clinical advantages and disadvantages.

Modality	**Advantages**	**Disadvantages**
Color Duplex Ultrasound (Smit et al., 2010)	non-invasive, applies to all sites, direct monitoring	Expensive, experienced personnel.
Fluorescein (Swartz et al., 1988; Graham et al., 1983; Furnas and Rosen, 1991; Chowdary et al., 1987)	inexperienced personnel, rapid	unreliable, indirect monitoring, only cutaneous flaps and replants, undesirable side effects to fluorescein
Laser Doppler Flowmetry (Swartz et al., 1988; Smit et al., 2010)	low cost, continuous, non-invasive	limited penetration depth, slightly experienced personnel
Microdialysis (Smit et al., 2010)	applies to all sites	expensive, invasive, experienced personnel, indirect monitoring
Microendoscopy (Upile et al., 2006)	direct monitoring	expensive, cumbersome
Near-Infrared Spectroscopy (Smit et al., 2010; Lohman et al., 2013)	inexperienced personnel, non-invasive	moderately expensive, slow response, limited penetration depth, interference from ambient light
Photoplethysmography (Swartz et al., 1988; Furnas and Rosen, 1991)	non-invasive	no quantitative information, only cutaneous flaps, unreliable for dark skin
Positron Emission Tomography (Schrey et al., 2008)	direct monitoring, includes buried flaps	cumbersome, expensive
Thermocouple (Swartz et al., 1988; Furnas and Rosen, 1991)	continuous	no quantitative information, indirect monitoring, can't monitor muscle perfusion
Transcutaneous Po_2 (Swartz et al., 1988; Schrey et al., 2008)	inexperienced personnel	no quantitative information, indirect monitoring, invasive
Wired Implantable Doppler (Smit et al., 2010)	low cost, inexperienced personnel, applies to all sites, direct monitoring	invasive, prone to unreliability, foreign material
Wireless Implantable Doppler (Smit et al., 2010)	inexperienced personnel, applies to all sites, direct monitoring	invasive, size, foreign material

Table 2: Summary of Reported WID device accuracy.

Config.	Year & Reference	Accuracy	Technical Notes
CW	1978 (Di Pietro and Meindl, 1978)	±20% from theory	any vessel size and any flow profile; mean Doppler shift by ZCC
	1992 (Yonezawa et al., 1992)	linearity was within ±1% to the actual average flow velocity over measured range	directional; 20 cm/s − 150 cm/s tested flow rate range
	2004 (Vilkomerson and Chilipka, 2004), 2008 (Vilkomerson et al., 2008)	average blood flow velocity accuracy error less than 5%	directional; using diffraction grating transducers (DGT)
	2012 (Cannata et al., 2012)	average blood flow velocity accuracy errors less than 6%; peak blood flow velocity measurement deviating only 1.7% from measurements performed with a duplex ultrasound system	directional; using diffraction grating transducers (DGT)
	2014 (Tang et al., 2014)	< 6% deviation	directional; one measurement; reported 22.6 cm/s compared to true 24 cm/s flow
	2014, 2015 (Gimbel et al., 2014; Unadkat et al., 2014, 2015), 2016 (Rothfuss et al., 2016)	< ±5% above 8.00 mL/min; between -0.8% and +1.2% at largest calibrated flow rate	nondirectional; binary flow/no-flow scenarios measured
PW	1974 (Hartley and Cole, 1974)	reported as accurate up to 100 ml/min flows	directional; transcutaneously excited probe (i.e., no implanted electronics)
	1975 (Gill and Meindl, 1975)	±15% blood flow volume estimation	nondirectional
	1977 (Allen et al., 1977)	+2.0 ±8.7%	nondirectional; 77 trials

Table 3: Summary of Reported WIDs with reported Implant Size and Miniaturization Technique.

Year & Reference	Reported Implant Size	Miniaturization Technique
1974 (Hartley and Cole, 1974)	3 cm diameter coil (only reported coil size)	inductively coupled to transducer (all electronics external)
1975 (Gill and Meindl, 1975)	60 cm^3, 20% by electronics	Custom Integrated Circuits; further demodulation and processing externally
1975 (Cathignol et al., 1975)	4 x 4 cm (only reported antenna size)	performing demodulation, filtering, processing externally
1978 (Allen et al., 1978)	3.8 x 2.8 x 0.8 cm implanted package	Custom Integrated Circuits; further demodulation and processing externally
1978 (Di Pietro and Meindl, 1978)	$<$ 36 cm^3; 6.1 x 4.1 x 1.3 cm (encapsulated electronics, battery, and antennas dimensions)	Custom Integrated Circuits
1989 (Yonezawa et al., 1989)	12.4 cm^3; 25 mm x 33 mm PCB	COTS parts; performing demodulation, filtering, processing externally
1992 (Yonezawa et al., 1992)	27 cm^3	COTS parts; performing demodulation, filtering, processing externally
2008 (Vilkomerson et al., 2008)	PCB_1: $\sim$3.5 x 5.5 cm; PCB_2: $\sim$2.5 x 4.9 cm	COTS parts; two PCBs; stacked; SMT
2012 (Cannata et al., 2012)	one board from (Vilkomerson et al., 2008)	COTS parts; SMT
2014 (Tang et al., 2014)	7 cm^2 (total PCB area)	COTS parts; two PCBs; SMT; performing demodulation, filtering, processing externally; small battery wirelessly recharged
2014, 2015, 2016 (Rothfuss et al., 2016; Gimbel et al., 2014; Unadkat et al., 2014, 2015)	1.7 cm^3 (electronics and antenna only); 18.04 cm^3 (encapsulated electronics, battery, and antennas)	COTS parts; 4-layer two-sided PCB; SMT

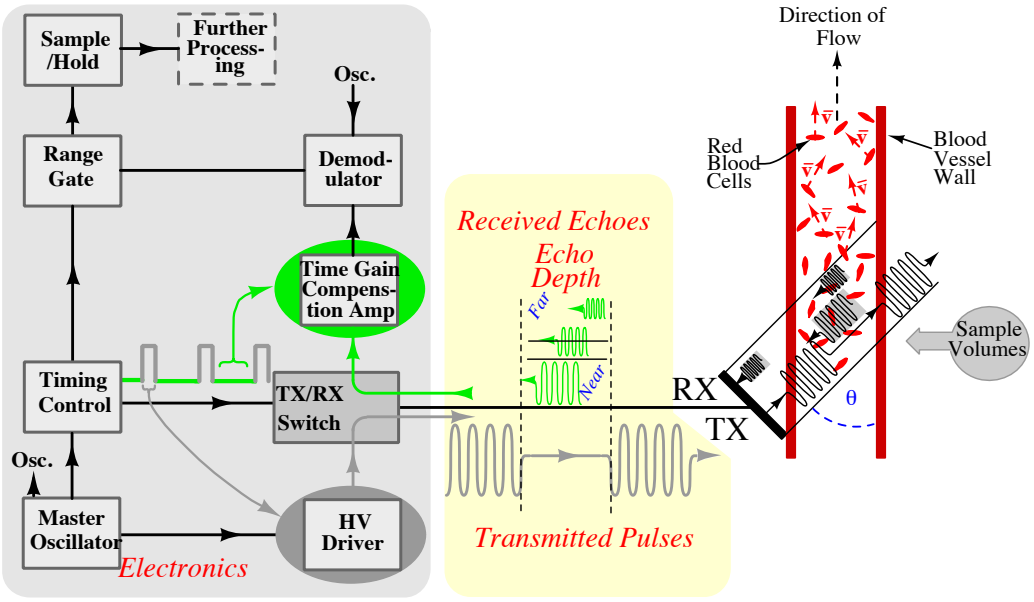

Figure 1: System-level block diagram of the nondirectional Pulsed Wave Doppler flowmeter. Adapted from (Shung, 2005; Boote, 2003; Brunner, 2002).

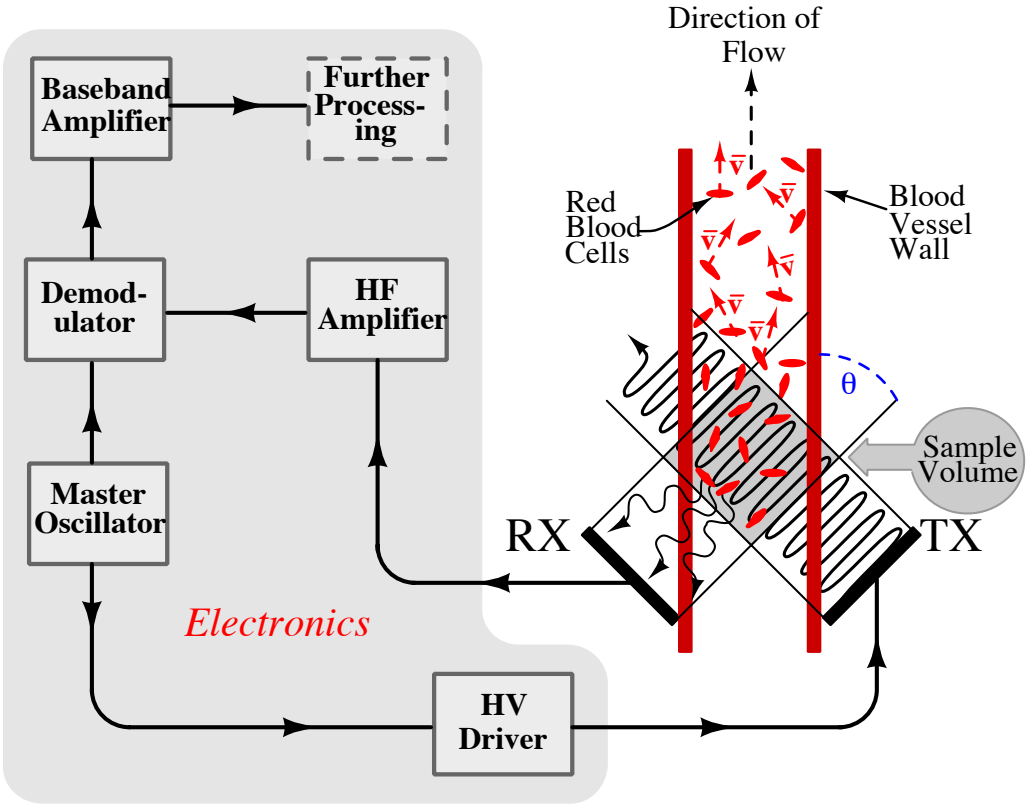

Figure 2: System-level block diagram of the nondirectional Continuous Wave Doppler flowmeter.